DIRECT-DRIVE AND EDDY-CURRENT SEPTUM MAGNETS

S. H. Kim
June 29, 2001

Abstract -- Two types of thin septum magnets, direct drive and eddy current, were compared mainly in 2-D magnetic aspects. For the direct-drive type, the leakage field depended on the finite permeability of the magnet core and not on the thickness of the septum conductor. It was suggested that the leakage field be controlled by reducing the current in the septum conductor or by using a correction coil. There were no significant differences between the two types regarding thermal problems caused by high current densities in the thin septa. The leakage fields with 2-mm septum thicknesses were calculated using OPERA-2d to compare the two types. For the eddy-current type, the leakage fields calculated using OPERA-2d were compared with the calculations from Halbach's model. The leakage fields for the eddy-current type decayed with long time constants.

1. Introduction

A septum magnet is a specially designed dipole magnet typically using a magnet core of C-shaped steel laminations. A "thin" septum separates two distinct regions of magnetic field, one a high gap field between the magnet poles to achieve a maximum deflection of charged particle beams during injection to or extraction from a circular accelerator, and one outside the septum that coincides with a "field-free" region of the circulating beam orbit. The essential features of a septum magnet are a spatially uniform gap field up to the inner surface of the septum, an acceptable apparent thickness of the septum region, and an extremely low magnetic field outside the septum (called "stray" or "leakage field"), in order not to affect the circulating beam.

Figure 1 schematically shows the cross section of a C-type dipole magnet with coil C and septum conductor S as the driving current coils. From Ampere's law the septum current density j (A/mm^2) in S is approximately given by $j = 10^{-3}\, B_o/(\mu_o\, d_1)$, where the gap field B_o is in teslas, the septum thickness d_1 in millimeters, and μ_o the permeability in vacuum. To achieve a gap field of 0.75 T, for example, the current density in the septum reaches $600/d_1$ (A/mm^2). High-current density in a thin septum results in a major thermal loading problem from ohmic heating in the septum. The septum magnetic field can be DC or pulsed. When the effects of the eddy currents in the magnet core are ignored, there will be no differences between the DC and pulsed ones as far as the magnetic flux distribution is concerned. However, because of the high thermal loading in the septum conductor, a DC septum is possible only when the required gap field is relatively low or the septum is relatively thick. Otherwise the magnet must be pulsed, and the duty factor of the septum must be adjusted to reduce the thermal loading to an acceptable level. There are two types of pulsed septum magnets: direct drive and eddy current (also known as transformer).

Keizer [1] has described the two-dimensional theory of direct-drive septum magnets. He has also discussed different septum geometries, the compensations of hysteresis, and finite permeability effects using back-leg windings. New developments in direct-drive pulsed septum magnets have successfully achieved the required magnetic specifications by using special designs for the cooling of the septum region [2,3]. An alternative design of the pulsed septum

is the eddy-current type: the driving coil is wound around the flux-return core, and the field-free region must be shielded from the gap field by the eddy currents in the septum conductor. Since there is not much space restriction on the thickness of the coil, one can choose a single-turn or multi-turn coil. Magnetic field measurements have shown that the peak of the leakage fields appears after the driving current pulse [4-6]. Halbach has analyzed a model for the eddy-current type and has shown that the decay of the leakage field has a relatively long time constant [7]. The model uses appropriate boundary conditions between the interfaces of the septum conductors and vacuum, and also uses Poynting's theorem, namely, the relationship between the rate of increase of the stored energy for the magnetic fields in the beam chamber outside the septum and the energy flow outward across the septum surface. The model neglects the ohmic heating in the septum conductor.

The purpose of this note is to compare the two types of pulsed thin-septum magnets, mainly in basic 2-D magnetic aspects. Numerical data, if not otherwise specified, are results from the electromagnetic calculations using OPERA-2d [8]. A driving current pulse of a half sine wave with a pulse width of 0.4 ms is used for the magnet calculations. In the following section, possible control of the leakage field is discussed for the direct-drive septum. In Section 3, decays of the leakage fields are compared to the calculation results from Halbach's model and OPERA-2d. Calculations of the magnetic field in iron laminations and leakage fields are summarized in Appendices A and B, respectively.

2. Direct-Drive Septum

For the upper half of the 2-D direct-drive septum magnet in Fig. 1 the septum conductor S is located in $-1.0 \le x \le 0$. The magnetic flux distribution was generated at the peak of a half-sine-wave current pulse. The weak leakage field outside of the magnet is not shown. When the field-decay time constant $\tau = \mu\sigma\, d_L^{\,2}$ for a lamination thickness $2d_L$ was comparable to the pulse width of the driving current, it was assumed that the effects of the eddy current in the laminations were negligible and that the flux distribution at the peak of the current pulse was no different from that of the static field. Ampere's law can then be applied to take a line integral of static magnetic field along a closed contour abdea (Fig. 1), and the leakage field integral outside the septum may be written as

$$\int_d^e B_s ds = \mu_o (I_c - I_s) - \int_a^d (B_s / \mu_r) ds, \tag{1}$$

where B_s is the magnetic field component parallel to ds; I_c and I_s are the driving currents in coil C and the septum conductor S, respectively; μ_r is the relative permeability for the magnet core; and the line integral path of B_s/μ_r is inside the magnet core. Since the currents in C and S generally have the same magnitude, the leakage field is determined by the integral B_s/μ_r in the magnet core and has nothing to do with the septum thickness. Therefore, in order to reduce the leakage field one must choose the steel laminations of high permeability and the cross section of the lamination core to be as large as possible. It should be noted from Eq. (1) and Fig. 1 that the leakage field outside the septum is always in the opposite direction of the main field in the gap.

Relying on the term B_s/μ_r for reducing the stray field has a certain limit. Increasing the cross section of the magnet core will not reduce the leakage field to an arbitrarily small value. But the leakage field may be reduced by (a) using correction coils (C1 and C2 in Fig. 1) of current ΔI with the same current direction in C1 and C, or by bypassing $-\Delta I$ from the septum

conductor to CS (for example, located on the top of the magnet as shown in Fig. 1) so that $\mu_o \Delta I$ cancels out the integral B_s/μ_r in Eq. (1), and (b) modifying the septum conductor geometry as shown in Fig. 2 to reduce the current density in the septum near the midplane. In the former case, the leakage field may be adjustable during operation or testing of the magnet; the latter case may depend on careful design of the septum conductor. For a certain case of septum magnet fabrication, the septum conductor was spot-welded along the edge of the magnet core to reinforce the mechanical stability of the septum. When steel bars were used along the length of the magnet core assembly, a fraction of the septum current bypassed to the steel bars. This reduced the leakage field or reversed the field direction, depending on the fraction of the bypass current.

The leakage fields calculated with a few different configurations of septum geometries and currents are plotted in Fig. 3. Typical permeability values of "1010 steel" for the magnet core were used for the calculations. When the 1-mm septum conductor was located in $-1.0 \le x \le 0$ for the magnet core geometry of Fig. 1, the leakage field was approximately -1 mT for the gap field of 0.75 T. By diverting 0.16% of the current in the septum to CS, the leakage field was nearly cancelled with the line integral term B_s/μ_r. When the septum geometry of Fig. 2 was used, the leakage field was -0.43 mT with the septum current of 0.3% diverted to S2 and was +0.45 mT with 0.76% to S2. The "air" gap between the septum and the magnet core also changes the leakage field due to the changes in the flux path and the current density in the septum. For a gap of 0.3 mm, which increases the effective current density by 2.7%, the leakage field was -8 mT. Since the total septum current in S1 and S2 remained unchanged, different values of the leakage fields near the septum converged to a single value, roughly -1 mT, at a larger distance from the septum, as expected from Eq. (1).

In Appendix A, the time response of the magnetic field in the steel lamination to the driving current was calculated assuming: (a) the magnetic field at the edge of the lamination follows the time response of the current pulse, and (b) the average field in the lamination follows it. In Fig. 4, the edge field and average field for lamination thicknesses of 0.18 mm ($\omega_o \tau = 1.63$) and 0.36 mm ($\omega_o \tau = 6.52$) are plotted from Eqs. (A8) and (A11). Since the relative permeability of the core was on the order of 10^3 compared to the unity in the space between the laminations, the magnitude of the gap field was assumed to be the same as that of the average field in the lamination. According to the measurement data of the septum magnets for the APS, which used 0.36-mm laminations, the time response of the gap field was very close to those of the driving current with a pulse-width of roughly 0.4 ms. To avoid field saturation at the edge of the lamination and to avoid the delay of the leakage field after the current pulse, it may be necessary to keep $\omega_o \tau$ less than 2.

3. Eddy-Current Septum

The cross section for the upper part of an eddy-current septum magnet is schematically shown in Fig. 5 without shielding the magnet core. The current in the septum conductor for the direct-drive septum magnet now flows in the coil CB at the backside of the magnet core. The magnetic flux generated by the current in CB did not change the flux distribution near the septum area. It only reduced the gap field slightly by reducing the permeability of the magnet core. Roughly 45% of the magnetic flux was leaked to the outside of the magnet (27% to the front side), when the core was not shielded. Figure 6 shows the vertical fields calculated near the midplane of the magnet without the septum. The driving current in CB did not change the

fields. By the method of conformal transformation the vertical field may be calculated approximately by using $\mu_r = \infty$ for the magnet core

$$B = B_o \frac{1}{[1+\exp(\pi\xi)]^{1/2}}, \tag{2}$$

where B_o = 0.75 T and $B = 0.833B_o$ at $x = 0$ (which corresponds to $\xi = -0.261$). An eddy-current septum has a burden to shield nearly all the magnetic flux for $0 \le x$ in Fig. 6 by inducing eddy currents near the $x = 0$ plane.

Figure 7(a) shows the flux distribution for a half-sine-wave current pulse at the peak of the current (0.2 ms); the relatively low leakage field compared to the gap field is not shown. Figure 7(b) shows the flux distribution at the end of the pulse width (0.4 ms) when the gap field is nearly zero. The front of the magnet, except the septum area, was shielded with a high-conductive copper plate, and the septum was a Cu-Fe composite with a thickness of 2 mm. Details of the vertical fields near the midplane of the septum region during and after the current pulse are plotted in Fig. 8. In the steel part of the septum, the relative permeability varied between 45-167, depending on the location and time. The time constants calculated for copper and steel with μ_r = 100 were 0.064 ms and 0.64 ms, respectively. At the peak of the current pulse, 0.2 ms, when the field did not penetrate the steel part of the septum completely, the leakage field was relatively low. At this time, the eddy current in the septum was approximately 98% of the peak driving current when a return path for the eddy current was allowed for efficient shielding of the gap field. At the end of the current pulse, the leakage field reached a peak and began to decay. The figure also shows that the field penetration in the steel was nearly complete at 0.4 ms, and from 0.6 ms it began to decay from the peak field over 2 T. The field decay slowed down as the permeability increased at a lower field. After 1.5 ms the leakage field remained at 0.017 T, and the magnetic field in the steel part of the septum only decayed less than 10% of its peak value. Results of similar calculations for a 2-mm Cu septum are plotted in Fig. 9. The time constant calculated for the copper was approximately 0.26 ms. The magnetic field in the Cu septum decayed out after 0.4 ms, but the leakage field remained at 0.033 T after 1.5 ms.

The leakage fields as a function of time from the start of the current pulse are plotted in Fig. 10 for several cases of 2-mm septa. The data for tr0 were calculated from Eq. (B6) of Halbach's model for a Cu septum with $a_1 = 10$, where $a_1 = D/d_1$ is the ratio of chamber width to septum thickness. Calculations from the model also show that when the time constant τ_1 for a copper septum is larger than the current pulse width t_o, the peak of the leakage field appears just after τ_1, and for τ_1 smaller than t_o, the peak appears at (0.5~1)t_o. The data for tr2 and tr4 in Fig. 5 were calculated for a Cu septum with and without beam chamber ($a_1 = 10$), respectively. The data for tr3 were calculated for a Cu-Fe septum with $\mu_r = 20$ and $a_1 = 20$, and those for tr5 are nonlinear calculations for the septum without beam chamber. The data, except for tr0, were calculated using OPERA-2d [8].

The dominant term of the leakage field $B(t)$ in Eq. (B6) calculated from Halbach's model for $t_o \le t$ is given by

$$B(t) \approx \frac{2a_1^{1/2}}{s_o + 1/s_o} \frac{(1+e^{s_o\omega_o t_o})e^{-s_o\omega_o t}}{(1+2a_1)\sin(a_1^{-1/2})}, \tag{3}$$

where $s_o = 1/(\omega_o \tau_1 a_1)$ with $\tau_1 = \mu_1 \sigma_1 d_1^2$. Equation (3) roughly follows $1/(\omega_o\tau_1 a_1)\exp[-t/(\tau_1 a_1)]$ when s_o has a value of much less than 1. From an approximate calculation for a Cu-Fe septum,

Halbach has concluded that the results for the pure Cu septum apply to the Cu-Fe septum when the iron has zero conductivity and a_1 is replaced by $(D + \mu_r d_2)/d_1$, where d_2 is the thickness of the iron. For D = 20 mm, μ_r = 20, and d_1 and d_2 = 1.0 mm (data tr2 and tr3 in Fig. 10), a_1 = 40. The time constant τ_1 = 0.26 ms for the 2-mm Cu is reduced to 0.065 ms for the 1-mm Cu. This makes $\tau_1 a_1$ unchanged from that of tr0 in Fig. 10, which may be interpreted as the magnetic flux in the steel sheet d_2 being evenly distributed in $\mu_r d_2$.

4. Conclusions

For the direct-drive septum magnet, the leakage field depends on the finite permeability of the magnet core, not on the septum thickness, and may be reduced by adjusting the current $(I_c - I_s)$ in Eq. (1). Reducing the thermal loading and avoiding cyclic fatigue in thin septa remain major problems for long-term stable operations. For the eddy-current type, the induced eddy current in the septum was 98% of the peak driving current, and a return path of the eddy current should be allowed for efficient shielding of the leakage field. Therefore, mechanical and thermal problems due to the high current density in the thin septum should not be different between the two types. For the eddy-current type, the peak of the leakage field appears after the driving current pulse. Calculations of the leakage fields from Halbach's model and OPERA-2d agreed fairly well for a ratio of the chamber dimension to the septum thickness of 10. When the time constant τ_1 for a copper septum was larger than the current pulse width t_o, the peak of the leakage field appeared just after τ_1, which is the time delay for the flux penetration through the septum. For τ_1 smaller than t_o, the peak appeared at $(0.5\text{-}1)t_o$. Generally, the results from OPERA-2d were not very sensitive to the chamber dimensions.

Appendix A. Magnetic Fields in Steel Laminations

Steel laminations of thickness $2d_L$, separated by the space between the laminations, are drawn schematically in Fig A1. The dimensions of the laminations were assumed to be much larger than that of the thickness. It was also assumed that the applied magnetic field B by a current pulse of a half sine wave and the induced electric field E in the laminations are in the y- and z-directions, respectively, and B and E depend only on the coordinate x and time t. Then, Maxwell's equations

$$\nabla \times \vec{E} = -\frac{\partial \vec{B}}{\partial t}, \qquad \nabla \times \vec{H} = \sigma \vec{E}, \tag{A1}$$

may be combined to make the diffusion equation for the magnetic field in the lamination

$$\frac{\partial^2 B(x,t)}{\partial x^2} = \mu\sigma \frac{\partial B(x,t)}{\partial t}, \tag{A2}$$

where σ is the conductivity of the lamination, and the permeability of the lamination $\mu = \mu_o \mu_r$ is assumed to be constant. The Laplace transform (LT) of Eq. (A2) and its solution is given by

$$\frac{d^2 B(x,p)}{dx^2} = \mu\sigma p B(x,p), \tag{A3}$$

$$B(x,p) = B_o(d_L,p)\frac{\cosh \xi x/d_L}{\cosh \xi}, \tag{A4}$$

where p is the parameter for the LT, $B_o(d_L, p)$ is the field at the edge of the lamination, and $\xi \equiv \sqrt{\tau p}$ with $\tau = \mu\sigma {d_L}^2$ as the time constant for the lamination. From Eq. (A4), the average field $\bar{B}(p)$ across the lamination thickness may be calculated as

$$\bar{B}(p) = B_o(d_L, p)\frac{\sinh\xi}{\xi\cosh\xi}. \tag{A5}$$

The inverse LT of Eq. (A5) depends on whether we know the average field or the edge field. If we assume that the field in the space between the laminations follows the time response of the driving current of a half sine wave with a pulse width of t_o ($\omega_o = \pi / t_o$),

$$\begin{aligned} &B(|x| \ge d_L, t) = B_{oo}\sin\omega_o t, \ (0 \le t \le t_o) \\ &B(x, +0) = 0, \end{aligned} \tag{A6}$$

then $B_o(d_L, p)$ in Eq. (A5) may be substituted with the LT of Eq. (A6),

$$B_o(d_L, p) = B_{oo}\frac{\omega_o}{\omega_o^2 + p^2}(1 + e^{-\pi p/\omega_o}). \tag{A7}$$

Equation (A5) then has poles at $p = \pm i\omega_o$ and $p = -\pi^2(m - 1/2)^2 / \tau$, $(m = 1, 2, 3, \cdots)$. The inverse LT of the average field is calculated to

$$\begin{aligned} \frac{\bar{B}(t)}{B_{oo}} &= \frac{1}{(\omega_o\tau)^{1/2}}\frac{(\cosh^2 2k - \cos^2 2k)^{1/2}}{\cosh 2k + \cos 2k}\sin(\omega_o t - \varphi) + \sum_{m=1}^{\infty}\frac{2}{\pi^2(m-1/2)^2}\frac{e^{-s_m\omega_o t}}{s_m + 1/s_m}, \ (0 \le t \le t_o) \\ &= \sum_{m=1}^{\infty}\frac{2}{\pi^2(m-1/2)^2}\frac{1 + e^{s_m\pi}}{s_m + 1/s_m}e^{-s_m\omega_o t}, \quad (t \ge t_o) \end{aligned} \tag{A8}$$

with parameters $k = (\omega_o\tau/2)^{1/2}$, $s_m = \pi^2(m - 1/2)^2 / \omega_o\tau$, and $\tan\varphi = \dfrac{\sinh 2k - \sin 2k}{\sinh 2k + \sin 2k}$.

On the other hand, if we assume that the average field follows the driving current pulse:

$$\begin{aligned} &\bar{B}(t) = B_{oo}\sin\omega_o t, \ (0 \le t \le t_o) \\ &\bar{B}(p) = B_{oo}\frac{\omega_o}{\omega_o^2 + p^2}(1 + e^{-\pi p/\omega_o}), \end{aligned} \tag{A9}$$

then instead of Eq. (A5), we solve the edge field $B_o(p)$ from

$$B_o(p) = \bar{B}(p)\frac{\xi\cosh\xi}{\sinh\xi}. \tag{A10}$$

The poles of Eq. (A10) are at $p = \pm i\omega_o$ and $p = -(n\pi)^2 / \tau$, $(n = 1, 2, 3, \cdots)$. With $s_n = (n\pi)^2 / \omega_o\tau$, the inverse LT of the edge field is given by

$$\begin{aligned} \frac{B(\pm d_L, t)}{B_{oo}} &= (\omega_o\tau)^{1/2}\frac{(\cosh^2 2k - \cos^2 2k)^{1/2}}{\cosh 2k - \cos 2k}\sin(\omega_o t + \varphi) + \sum_{n=1}^{\infty}\frac{-2}{s_n + 1/s_n}e^{-s_m\omega_o t}, \ (0 \le t \le t_o) \\ &= \sum_{n=1}^{\infty}\frac{-2}{s_n + 1/s_n}(1 + e^{s_n\pi})e^{-s_m\omega_o t}. \qquad (t \ge t_o) \end{aligned} \tag{A11}$$

Appendix B. Halbach's Model of the Leakage Field in an Eddy-Current Septum Magnet

Figure B1 schematically shows the permeability, conductivity, and thickness of a Cu-Fe septum, and D is the dimension of a beam chamber in the x-direction outside the septum for the calculation of the Halbach's model [7]. We will assume that the magnetic field and eddy current near or in the septum have only y- and z- components, respectively. For the Cu septum ($d_2 = 0$), the magnetic field across the septum may be solved from Eq. (A3):

$$\frac{d^2B(x,p)}{dx^2} = k_s{}^2 B(x,p), \qquad k_s{}^2 = \mu_1\sigma_1 p. \tag{B1}$$

From Eq. (B1) and $dB/dx = \mu_1\sigma_1 E$ we find the magnetic field and induced electric field are

$$B(x,p) = B_o(p)\cosh k_s x + E_o(p)\frac{\mu_1\sigma_1}{k_s}\sinh k_s x, \tag{B2}$$

$$E(x,p) = -B_o(p)\frac{k_s}{\mu_1\sigma_1}\sinh k_s x + E_o(p)\cosh k_s x, \tag{B3}$$

where $B_o(p)$ is the gap field of the septum magnet and $E_o(p)$ is the electric field on the inner surface of the septum. The fields outside of the septum, $B_1(x = d_1)$ and $E_1(x = d_1)$, may be obtained from Eqs. (B2) and (B3). Using Poynting's theorem of power flow in electromagnetic fields, B_1 and E_1 are related

$$-\frac{E_1 B_1}{\mu_o} g = \frac{\partial}{\partial t}\frac{B_1{}^2}{2\mu_o} gD, \tag{B4}$$

or $E_1 = -DpB_1$ after LT. Here g is the septum height (pole gap), and the ohmic heating in the septum is neglected. Then, from Eqs. (B2) and (B3) the leakage field may be expressed as

$$B(d_1,p) = B_o(p)/[\cosh\sqrt{\tau_1 p} + \frac{D}{d_1}\sqrt{\tau_1 p}\sinh\sqrt{\tau_1 p}], \tag{B5}$$

where $\tau_1 = \mu_1\sigma_1 d_1{}^2$ is the time constant of the septum conductor. If we assume that the gap field is the same as the average field in the steel laminations in its magnitude and time response, $B_o(p)$ may be replaced with Eq. (A9). Equation (B5) has poles at $p = \pm i\omega_o$, $p = -1/\tau_1 a_1$, and $p = -(n\pi)^2(1 + a_1^{-1}(n\pi)^{-2})^2/\tau_1$ with $a_1 = D/d_1$. Then, the inverse LT of Eq. (B5) is calculated as

$$\begin{aligned} B(t) &= \frac{1}{(P_1^2 + Q_1^2)^{1/2}}\sin(\omega_o t - \phi) + \frac{2a_1^{1/2}}{s_o + 1/s_o}\frac{e^{-s_o\omega_o t}}{(1+2a_1)\sin(a_1^{-1/2})} \\ &\quad + \sum_{n=1}^{\infty}\frac{2(-1)^n}{n\pi}\frac{1}{s_n + 1/s_n}\frac{e^{-s_o\omega_o t}}{\{1 + a_1 + (a_1 n\pi)^2\}\sin(1/a_1 n\pi)}, \quad (0 \le t \le t_o) \\ &= \frac{2a_1^{1/2}}{s_o + 1/s_o}\frac{(1 + e^{s_o\omega_o t_o})e^{-s_o\omega_o t}}{(1+2a_1)\sin(a_1^{-1/2})} \\ &\quad + \sum_{n=1}^{\infty}\frac{2(-1)^n}{n\pi}\frac{1}{s_n + 1/s_n}\frac{(1 + e^{s_n\omega_o t_o})e^{-s_o\omega_o t}}{\{1 + a_1 + (a_1 n\pi)^2\}\sin(1/a_1 n\pi)}, \quad (t \ge t_o) \end{aligned} \tag{B6}$$

with parameters

$$P_1 = \cosh k_1 \cos k_1 + a_1 k_1 (\sinh k_1 \cos k_1 - \cosh k_1 \sin k_1),$$
$$Q_1 = \sinh k_1 \sin k_1 + a_1 k_1 (\sinh k_1 \cos k_1 + \cosh k_1 \sin k_1),$$
$$k_1 = (\omega_o \tau_1 / 2)^{1/2}, \ \tan\phi = Q_1 / P_1, \ s_o = 1/(\omega_o \tau_1 a_1), \text{ and } s_n = (n\pi)^2 / (\omega_o \tau_1), \ (n = 1, 2, \cdots).$$

References

[1] R.L. Keizer, "Dipole Septum Magnets," CERN 74-13, Geneva, Switzerland (1974).

[2] M. Modena, H. Hsieh and C. Sanelli, "High Current Density Septum Prototype for Accumulator and Storage Ring of DAΦNE, the Frascati Φ–Factory," Proc. 4th EPAC, p. 2403 (1994).

[3] S. Sheynin, F. Lopez and S. Milton, "The APS Direct-Drive Pulsed Septum Magnets," Proc. 1995 Particle Accelerator Conf., p. 1355 (1995).

[4] K. Kumagai and S. Matsui, "The Injection Septum Magnets for the Spring-9 Storage Ring," *IEEE Trans. on Magnetics*, Vol. 30, p. 2134 (1994).

[5] F. Lopez, F. Mills, S. Milton, S. Reeves, S. Sheynin, K. Thompson and L. Turner, "The APS Thin Pulsed Septum Magnets," Proc. 4th EPAC, p. 2406 (1994).

[6] F. Rohner, "Magnetic Calculations on the Eddy Current Septum Magnet for the ESRF," ESRF Internal Note AT/MA/90-08 (1990).

[7] K. Halbach, "Some Thoughts on an Eddy Current Septum Magnet," Light Source Note LS-244, Argonne National Laboratory (1994).

[8] OPERA-2d, Vector Fields Ltd., Oxford, England.

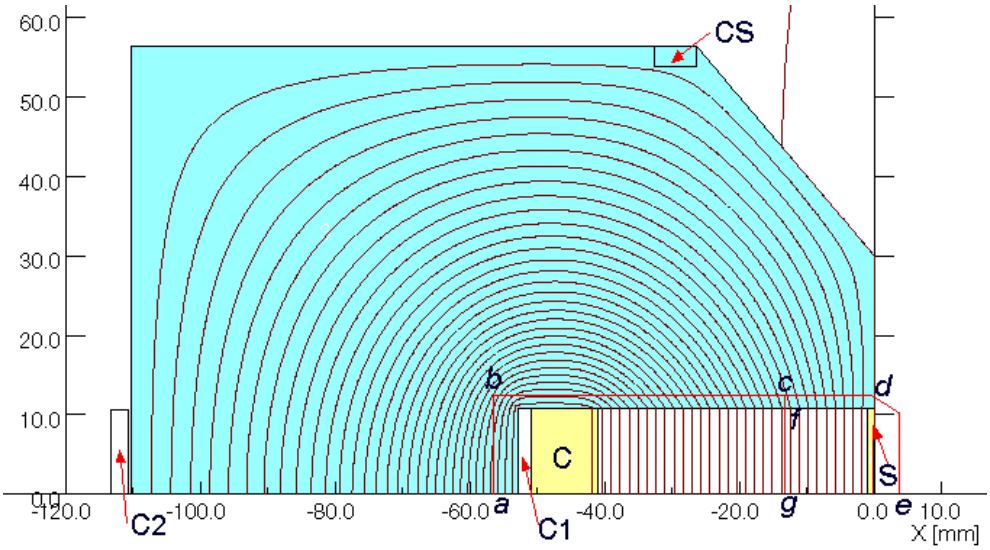

Fig. 1. Cross section of the upper half of a direct-drive septum magnet with its magnetic flux distribution. The relatively weak leakage field outside the septum is not shown. The main coil C and septum conductor S are used for driving current pulses of a half sine wave. The leakage field may be adjusted by bypassing a fraction of the current in the septum conductor to coil CS or by using correction coils C1 and C2. Lines abcd and de denote the line integral paths ad and de in Eq. (1), and gf is the half-gap of the magnet.

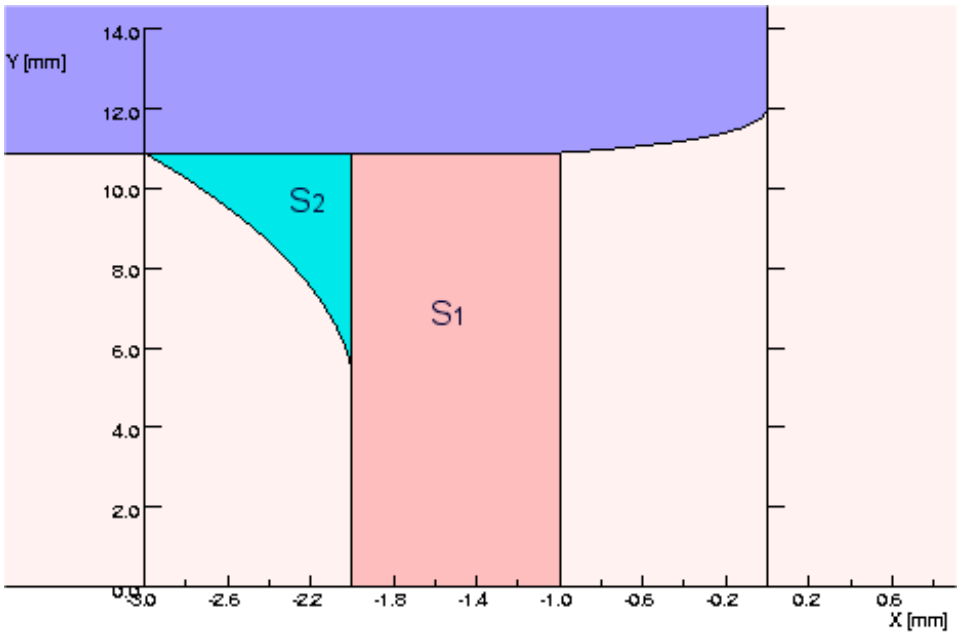

Fig. 2. The geometry of the septum cross section was modified by adding S2 to S1 for a direct-drive septum magnet. A small fraction of the driving current may be distributed in S2 to reduce the leakage field.

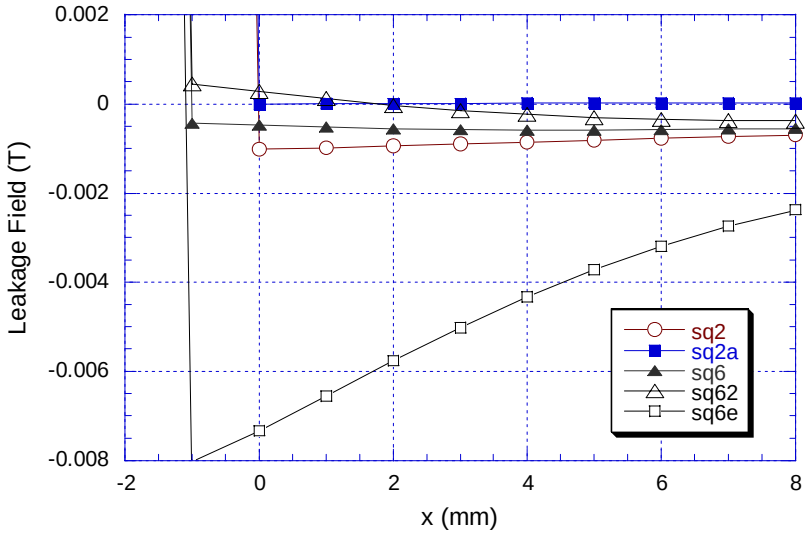

Fig. 3. Leakage fields of direct-drive septum magnets are plotted for five different cases of the septum. The outer surfaces of the septa were located at x = 0 for sq2 and sq2a, and x = –1.0 for sq6, sq62, and sq6e. The septum current I_s was varied: sq2 (I_s not changed); sq2a (0.16% of I_s bypassed to coil CS); sq6 (0.27% of I_s to S_2, shown in Fig. 2); sq62 (0.76% of I_s to S_2); and sq6e (0.3-mm air gap between the septum and magnet core).

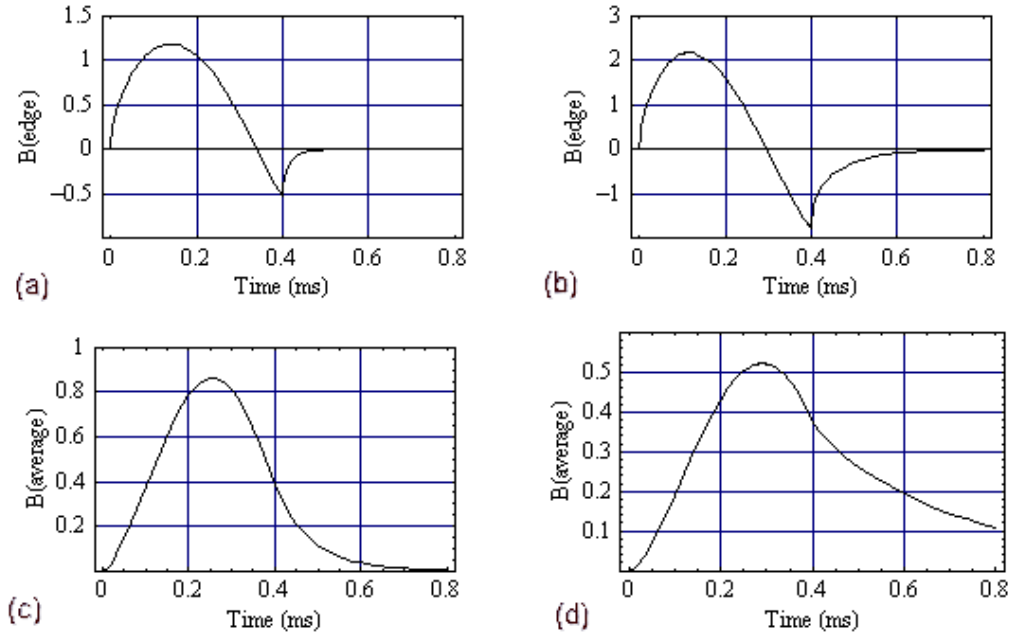

Fig. 4. Time responses of the magnetic field at the edge of steel lamination relative to the average field in the lamination are plotted from Eq. (A11) for lamination thickness (a) 0.18 mm ($\omega_b\tau$ = 1.63) and (b) 0.36 mm (($\omega_b\tau$ = 6.52). Time responses of the average fields in the laminations relative to the edge field are plotted from Eq. (A8) for lamination thickness (c) 0.18 mm and (d) 0.36 mm. The current pulse width and μ_r used for the plot were 0.4 ms and 4000, respectively.

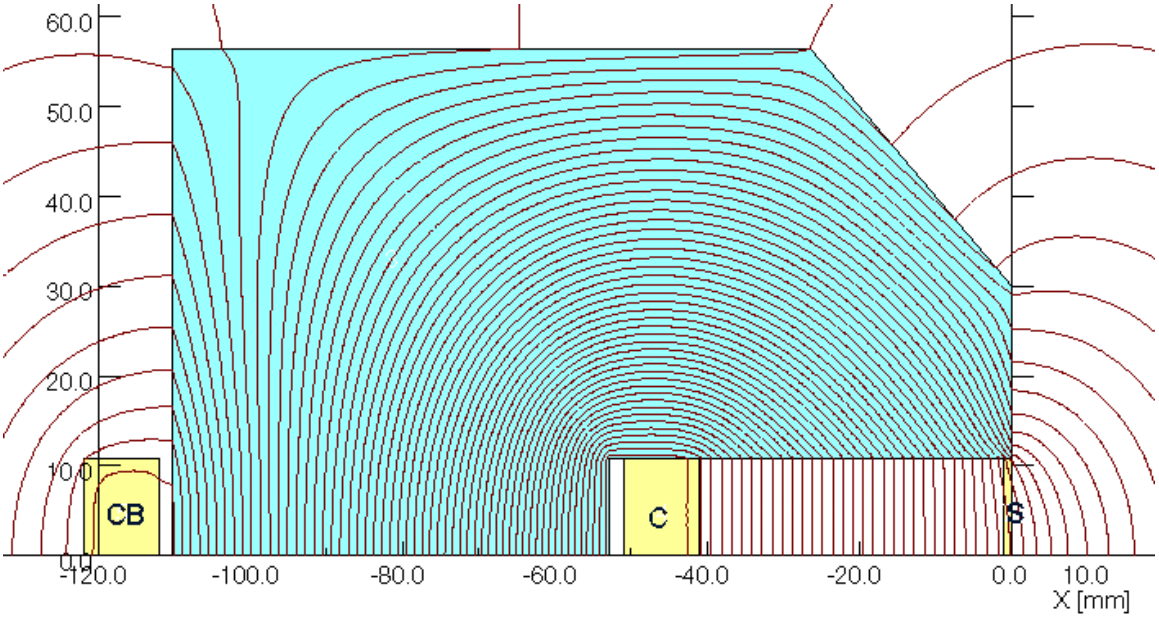

Fig. 5. Cross section for the upper part of an eddy-current septum magnet without the shielding of the magnet core. Current pulses of a half sine wave with a pulse width of 0.4 ms were driven by the main coil C and coil CB in the backside of the magnet. About 45% of the magnetic flux is scattered outside of the magnet.

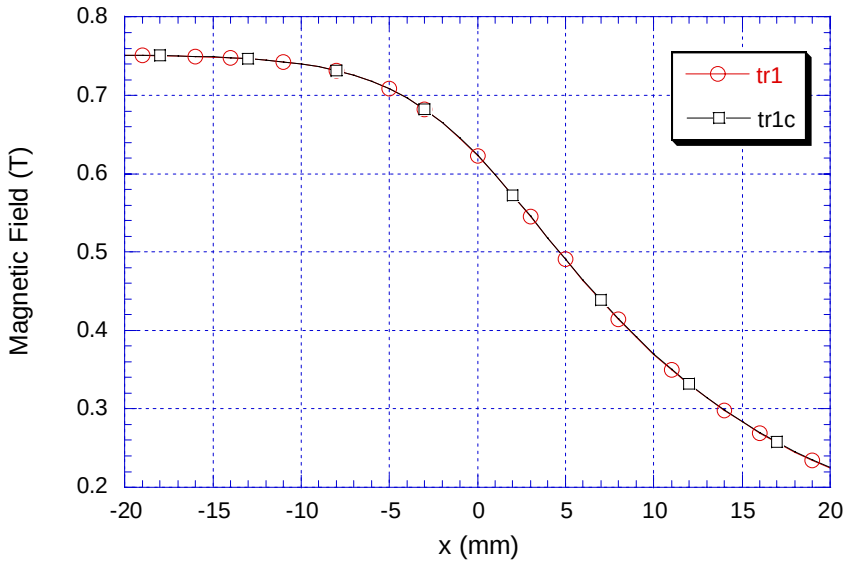

Fig. 6. Magnetic field calculated near the midplane of Fig. 5 at the peak of the driving current pulse with (tr1) and without (tr1c) coil CB. It was calculated without the septum and the shielding of the magnet core. The magnetic field at x = 0 was approximately 0.83% of the gap field 0.75 T.

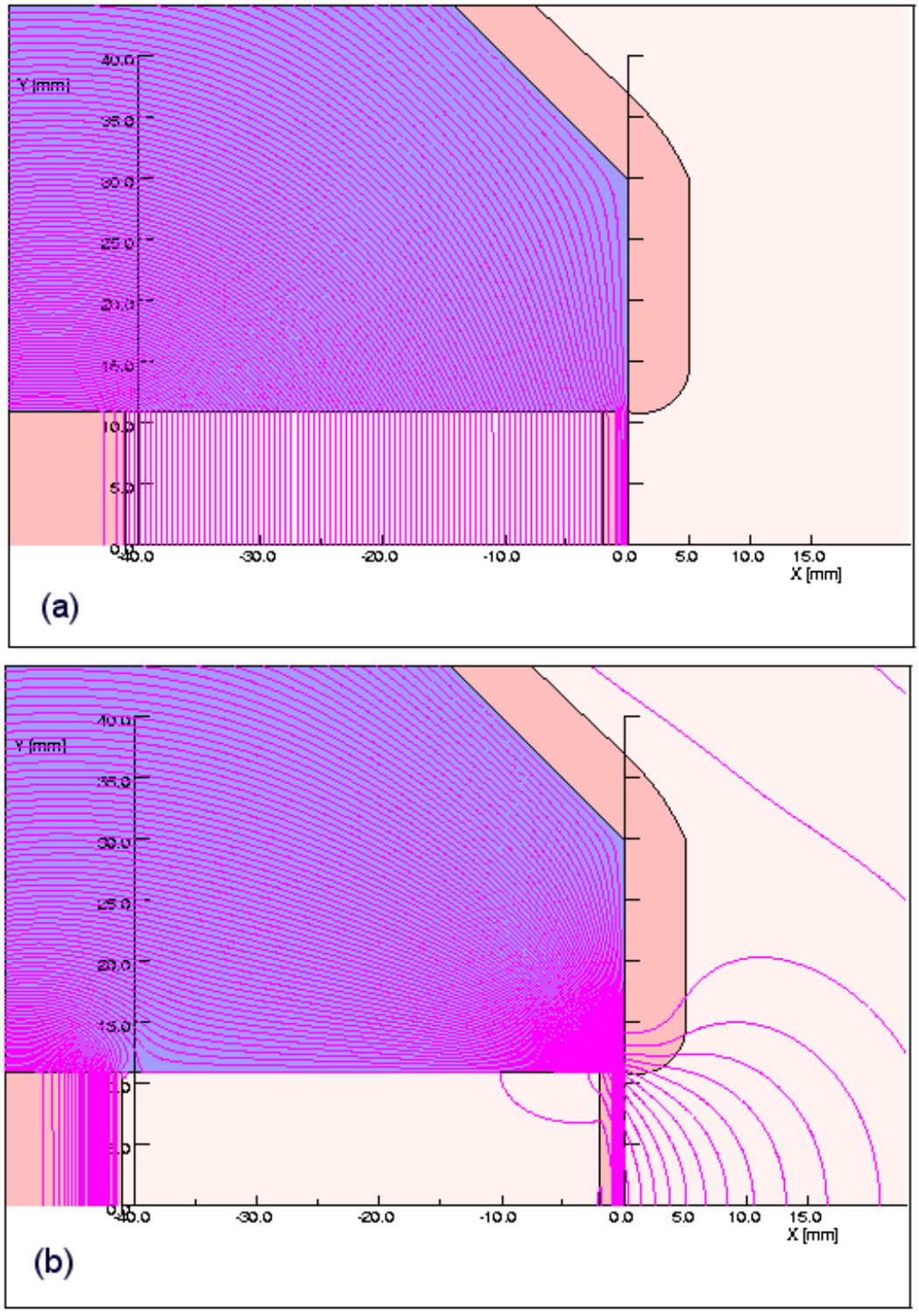

Fig. 7. Magnetic flux distribution for an eddy-current Cu-Fe septum magnet with shielding of the magnet core: (a) at the peak of the current pulse (0.2 ms) and (b) at the end of the pulse (0.4 ms) when the gap field is zero. The distribution of the relatively low leakage field compared to the gap field at 0.2 ms is not shown in (a).

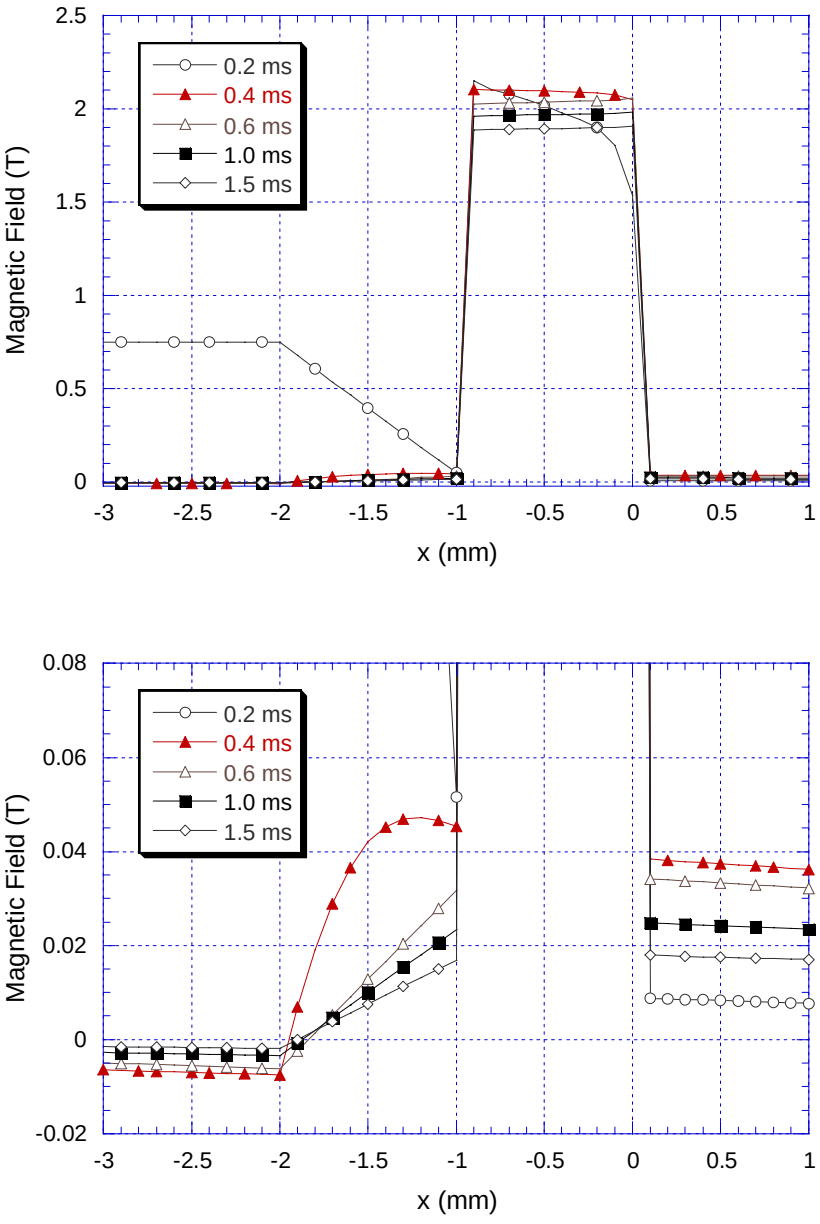

Fig. 8. Magnetic fields near the 2-mm Cu-Fe septum ($-2.0 \le x \le 0$) of an eddy-current septum magnet were calculated during and after the current pulse. The fields in the steel septum are over 2 T (*top*), and the leakage fields are shown in expanded scale for the vertical axis (*bottom*).

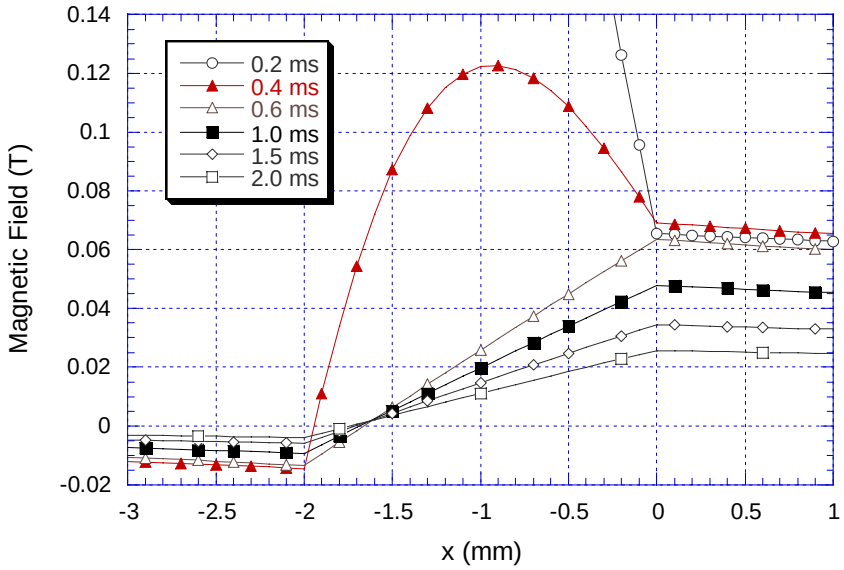

Fig. 9. Magnetic fields near a 2-mm Cu septum of an eddy-current septum magnet during and after a current pulse with a pulse width of 0.4 ms.

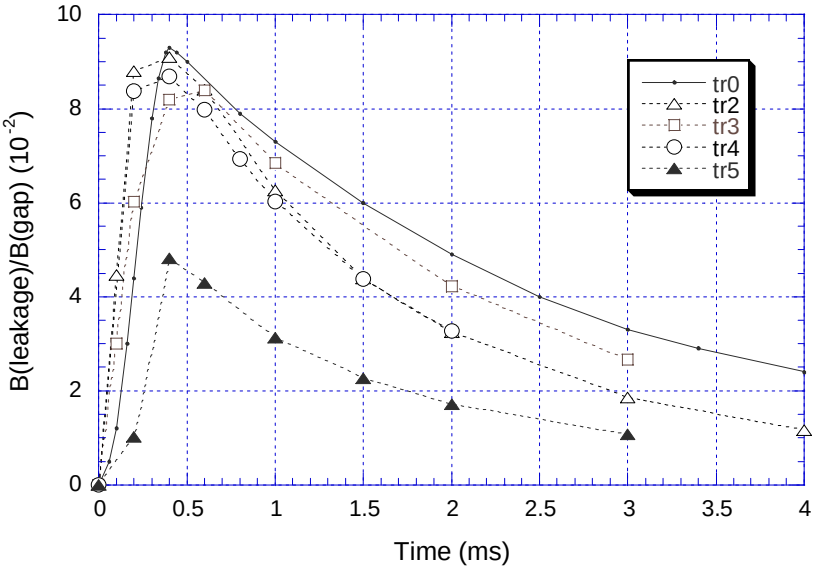

Fig. 10. Leakage fields for eddy-current septum magnets are plotted as a function of time from the start of the current pulse with $\omega_0\tau_1 = 2$ and 2-mm septa. tr0: Cu septum, calculated from Eq. (B6) for $a_1 = 10$. tr2: Cu septum for $a_1 = 10$. tr3: Cu-Fe septum for $\mu_r = 20$ and $a_1 = 20$. tr4: Cu septum without beam chamber. tr5: nonlinear calculation for Cu-Fe septum without beam chamber. OPERA-2d was used for all the calculations except tr0.

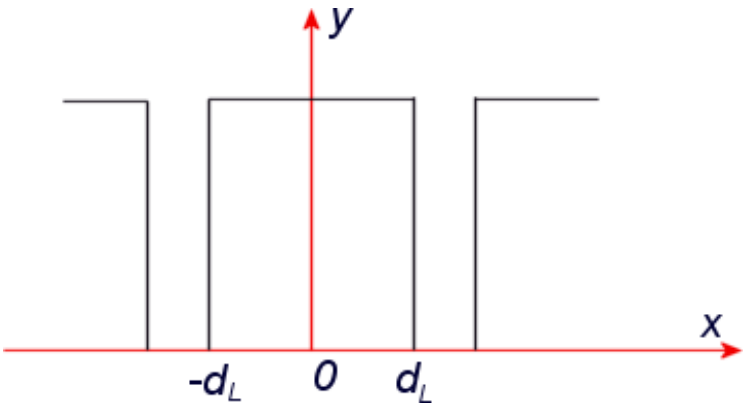

Fig. A1. Schematic drawing of steel laminations of thickness $2d_L$ are separated by "C5-coating" spaces.

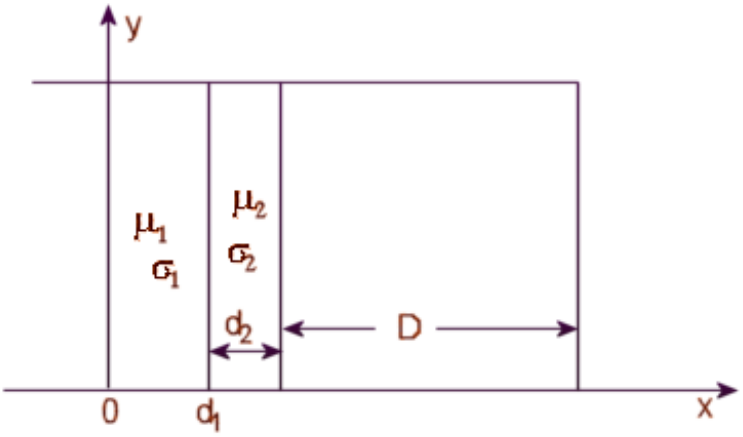

Fig. B1. Schematic drawing of two-component septum: subscripts 1 and 2 represent copper and iron, respectively, and D is the dimension of the beam chamber in the x-direction.